NLRP3 Inflammasome Activation Through Heart-Brain Interaction Initiates Cardiac Inflammation and Hypertrophy During Pressure Overload

Yasutomi Higashikuni, MD, PhD[1*], Wenhao Liu, MD[1], Genri Numata, MD, PhD[1], Kimie Tanaka, MD, PhD[1,2], Daiju Fukuda, MD, PhD[3], Yu Tanaka, MD, PhD[4], Yoichiro Hirata, MD, PhD[4], Teruhiko Imamura, MD, PhD[1,6], Eiki Takimoto, MD, PhD[1], Issei Komuro, MD, PhD[1], Masataka Sata, MD, PhD[5*]

1) Department of Cardiovascular Medicine, The University of Tokyo, 7-3-1 Hongo, Bunkyo-ku, Tokyo, 113-8655, Japan

2) Department of Clinical Laboratory Medicine, Juntendo University Graduate School of Medicine, 3-1-3 Hongo, Bunkyo-ku, Tokyo, 113-8431, Japan

3) Department of Cardio-Diabetes Medicine, Institute of Biomedical Sciences, Tokushima University Graduate School, 3-18-15 Kuramoto-cho, Tokushima-shi, Tokushima, 770-8503, Japan

4) Department of Pediatrics, The University of Tokyo, 7-3-1 Hongo, Bunkyo-ku, Tokyo, 113-8655, Japan

5) Department of Cardiovascular Medicine, Institute of Biomedical Sciences, Tokushima University Graduate School, 3-18-15 Kuramoto-cho, Tokushima-shi, Tokushima, 770-8503, Japan

6) Present affiliation: Second Department of Medicine, University of Toyama, 2630 Sugitani, Toyama-shi, Toyama, 930-0194, Japan

First author's surname: Higashikuni, **Short title**: Neural Control of Cardiac Inflammation

Word Counts: 5000 words

***Correspondence**:

Yasutomi Higashikuni, MD, PhD

7-3-1 Hongo, Bunkyo-ku, Tokyo 113-8655, Japan

Tel: +81-3-3815-5411, Fax: +81-3-5800-9171, Email: yasutomihigashikuni@g.ecc.u-tokyo.ac.jp

Or Masataka Sata, MD, PhD

3-18-15 Kuramoto-cho, Tokushima 770-8503, Japan

Tel: +81-88-633-7850, Fax: +81-88-633-7894, Email: masataka.sata@tokushima-u.ac.jp

ABSTRACT

BACKGROUND: Mechanical stress on the heart, such as high blood pressure, initiates inflammation and causes hypertrophic heart disease. However, the regulatory mechanism of inflammation and its role in the stressed heart remain unclear. Interleukin (IL)-1β is a proinflammatory cytokine that causes cardiac hypertrophy and heart failure. Here we show that neural signals activate the NLRP3 inflammasome for IL-1β production to induce adaptive hypertrophy in the stressed heart.

METHODS: C57BL/6 mice, knockout mouse strains for NLRP3 and P2RX7, and adrenergic neuron-specific knockout mice for SLC17A9, a secretory vesicle protein responsible for the storage and release of adenosine triphosphate (ATP), were used for analysis. Pressure overload was induced by transverse aortic constriction. Various animal models were used including pharmacological treatment with apyrase, lipopolysaccharide, 2'(3')-O-(4-benzoylbenzoyl)-ATP, MCC950, anti-IL-1β antibodies, clonidine, pseudoephedrine, isoproterenol, and bisoprolol, left stellate ganglionectomy, and ablation of cardiac afferent nerves with capsaicin. Cardiac function and morphology, gene expression, myocardial IL-1β and caspase-1 activity, and extracellular ATP level were assessed. *In vitro* experiments were performed using primary cardiomyocytes and fibroblasts from rat neonates and human microvascular endothelial cell line. Cell surface area and proliferation were assessed.

RESULTS: Genetic disruption of NLRP3 resulted in significant loss of IL-1β production, cardiac hypertrophy, and contractile function during pressure overload. A bone marrow transplantation experiment revealed an essential role of NLRP3 in cardiac non-immune cells in myocardial IL-1β production and cardiac phenotype. Pharmacological depletion of extracellular ATP or genetic disruption of the P2X7 receptor suppressed myocardial NLRP3 inflammasome

activity during pressure overload, indicating an important role of ATP/P2X7 axis in cardiac inflammation and hypertrophy. Extracellular ATP induced hypertrophic changes of cardiac cells in an NLRP3 and IL-1β-dependent manner *in vitro*. Manipulation of the sympathetic nervous system suggested sympathetic efferent nerves as the main source of extracellular ATP. Depletion of ATP release from sympathetic efferent nerves, ablation of cardiac afferent nerves, or a lipophilic β-blocker reduced cardiac extracellular ATP level, and inhibited NLRP3 inflammasome activation, IL-1β production, and adaptive cardiac hypertrophy during pressure overload.

CONCLUSIONS: Cardiac inflammation and hypertrophy are regulated by heart-brain interaction. Controlling neural signals might be important for the treatment of hypertensive heart disease.

Clinical Perspective:

What Is New?

- The nervous system controls cardiac inflammation and hypertrophy during pressure overload through NOD-like receptor pyrin domain-containing protein 3 inflammasome activation.
- Extracellular adenosine triphosphate released from sympathetic efferent nerve terminals activates the NOD-like receptor pyrin domain-containing protein 3 inflammasome in cardiac non-immune cells through stimulation of the P2X7 purinergic receptor.
- Pressure overload is sensed by cardiac afferent nerves to activate sympathetic efferent nerves for adenosine triphosphate release.

What Are the Clinical Implications?

- Controlling neural signals might have therapeutic potential for the treatment of hypertensive heart disease.
- Lipophilic β-adrenergic receptor blockers might act on the brain, as well as on the heart, to inhibit signals of the sympathetic nervous system and cardiac inflammation with its ability to cross the blood-brain barrier.
- Our mechanism might link psychological distress to heart disease.

INTRODUCTION

Cardiac hypertrophy occurs as an adaptive response to pathological stimuli to maintain cardiac function through reduction in wall stress and energy expenditure.[1] However, persistent stress responses lead to contractile dysfunction and heart failure.[2] Although inflammation is involved in these processes,[3] very little is known about the mechanism that controls cardiac inflammation and hypertrophy.

Inflammation is a complex process in which both immune cells and non-immune cells are involved. Proinflammatory cytokines, including interleukin (IL)-1β, IL-6, and tumor necrosis factor-α (TNF-α), induce cellular responses, such as cardiomyocyte hypertrophy, and fibroblast and immune cell activation, that lead to cardiac hypertrophy and heart failure.[3] It has been reported that non-immune cells, including cardiomyocytes, initiate inflammation by recognizing the endogenous molecules termed danger-associated molecular patterns (DAMPs) in the stressed heart, such as heat shock proteins and mitochondrial DNA, through innate immune receptors such as Toll-like receptors (TLRs).[4,5] Innate immune receptor signaling activates the transcription factor nuclear factor-kappa B (NF-κB) for the expression of proinflammatory cytokines, which activate NF-κB again via their receptors in an autocrine and paracrine manner for further inflammatory responses.[6] Immune cells such as macrophages and lymphocytes interact with proinflammatory cytokines to modulate their expression pattern.[7-9]

The nucleotide-binding domain, leucine-rich-containing family, pyrin domain-containing 3 (NLRP3) inflammasome is a cytosolic multiprotein complex that mediates active IL-1β production.[10] IL-1β is a proinflammatory cytokine that is critically involved in the pathophysiology of hypertrophic heart disease.[4,11] This complex consists of the Nod-like receptor family protein NLRP3, the apoptosis-associated speck-like protein containing a C-terminal

caspase recruitment domain (ASC), and procaspase-1. These components are upregulated through the activation of NF-κB, which is called NLRP3 inflammasome priming. Upon activation of NLRP3 by exogenous pathogens or endogenous danger signals, procaspase-1 is cleaved into 10kDa and 20kDa subunits to form the active enzyme, caspase-1. Subsequently, caspase-1 cleaves inactive pro-IL-1β into active IL-1β. Although the NLRP3 inflammasome in immune cells and non-immune cells has been implicated in cardiovascular stress and disease,[9,12-17] how it is activated and contributes to cardiac hypertrophy remain poorly understood.

Here we show that neural signals contribute to NLRP3 inflammasome activation in cardiac non-immune cells, which initiates inflammation and the adaptive programs in the stressed heart through IL-1β production. We find that pressure overload to the left ventricle activates sympathetic efferent nerves (SENs) to secrete extracellular adenosine triphosphate (ATP). Extracellular ATP stimulates the P2X7 purinergic receptor for NLRP3 inflammasome activation in cardiomyocytes, fibroblasts, and vascular endothelial cells. This mechanism is essential for IL-1β production, which causes cardiac adaptive hypertrophy in response to mechanical stress. We also demonstrate that cardiac afferent nerve signals contribute to ATP secretion from SEN terminals. These data collectively reveal that cardiac inflammation and hypertrophy are controlled via heart-brain interaction.

METHODS

For detailed description of Methods, please see the Supplemental Material. The data that support the findings of this study are available from the corresponding author upon reasonable request.

Animal Study

All experiments were approved by the University of Tokyo Ethics Committee for Animal Experiments, and strictly adhered to the guidelines for animal experiments of the University of Tokyo. Eight- to 12-week-old male mice were used. Wild-type C57BL/6 mice were purchased from Takasugi Experimental Animal Supply (Saitama, Japan). *Nlrp3*$^{-/-}$ mice were provided by the laboratory of Dr. Jurg Tschopp (The University of Lausanne, Switzerland).[18] *P2rx7*$^{-/-}$ and *Slc17a9*$^{flox/flox}$ mice were purchased from the Jackson Laboratory (Maine, USA). DBH-*Cre* mice were provided by RIKEN BRC through the National Bio-Resource Project of MEXT, Japan (Tsukuba, Japan).[19]

Pressure overload was induced by transverse aortic constriction (TAC) as described previously.[4] Apyrase (4 units, Sigma, St. Louis, Missouri, USA), lipopolysaccharide (LPS) (2mg/kg, InvivoGen, San Diego, California, USA), 2'(3')-O-(4-benzoylbenzoyl)-ATP (BzATP) (5mg/kg, Sigma), MCC950 (10mg/kg, Selleck Chemicals, Houston, Texas, USA), and clonidine (10μg/kg, Sigma) were injected intraperitoneally daily. Anti-IL-1 antibody or control antibody (100μg per mouse, R&D Systems, Minneapolis, Minnesota, USA) was injected intravenously. Pseudoephedrine (20mg/kg/day, Ieda Chemicals, Tokyo, Japan) and bisoprolol hemifumarate (5mg/kg/day, Tokyo Chemical Industry, Tokyo, Japan) were orally administered to mice by gavage daily. Isoproterenol (Sigma-Aldrich, St. Louis, Missouri, USA) was administered to mice via an osmotic minipump (30mg/kg/day, ALZET mini-osmotic pump, DURECT Corporation, Cupertino, California, USA). Left stellate ganglionectomy was performed just before TAC or sham operation.[20] To ablate primary afferent neurons, subepicardial injection of capsaicin (50mg/ml, Sigma) dissolved in olive oil (Wako, Osaka, Japan) was performed at 2 weeks before induction of TAC.[21]

148 **Human Samples**

149 The use of previously obtained human heart biopsy samples from heart failure patients for daily
150 practice was approved by the Institutional Review Board of the University of Tokyo Hospital,
151 and consent was obtained from all subjects. These samples were fixed in 10% formalin and
152 embedded in paraffin.

153

154 **Statistical Analyses**

155 Statistical analyses were performed with EZR (Saitama Medical Center, Jichi Medical
156 University, Saitama, Japan), which is a graphical user interface for R (The R Foundation for
157 Statistical Computing, Vienna, Austria).[22] Differences in means between two groups were
158 analyzed by unpaired two-tailed t-test. More than two groups were compared using one-way
159 analysis of variance (ANOVA) followed by Holm test or Dunnett's test for multiple comparison.
160 The Kaplan-Meier method with log-rank test was used for survival analysis. Values of $P<0.05$
161 were considered statistically significant.

162

163 **RESULTS**

164 **The NLRP3 Inflammasome Is Activated in the Stressed Heart**

165 To investigate the involvement of the NLRP3 inflammasome in hypertrophic heart disease, we
166 first examined gene and protein expression of NLRP3 inflammasome components and IL-1β,
167 and caspase-1 activity and cleavage in myocardial tissue. In wild-type mice, NLRP3 mRNA and
168 protein were upregulated during pressure overload caused by TAC (Figure 1A and Figure S1A
169 and S1B). Immunohistochemical staining demonstrated that NLRP3 is heterogeneously
170 expressed in both cardiomyocytes and non-cardiomyocytes in the murine pressure-overloaded

heart and the human failing heart (Figure 1B). Gene and protein expression levels of other inflammasome components, such as ASC and procaspase-1, and pro-IL-1β were also upregulated in the pressure-overloaded heart, indicating activation of priming signals (Figure S1). Caspase-1 activity and cleaved caspase-1 level were increased during pressure overload and peaked at day 14 after TAC (Figure 1C and Figure S1B). Protein expression of IL-1β was significantly increased during the adaptive hypertrophic phase until day 14 after TAC (Figure 1D). These results indicate that the NLRP3 inflammasome is activated in the stressed heart, especially during the adaptive hypertrophic phase.

Genetic Disruption of NLRP3 Inhibits IL-1β Production and Adaptive Cardiac Hypertrophy

To examine the role of the NLRP3 inflammasome in hypertrophic heart disease, we induced pressure overload by TAC in *Nlrp3*$^{+/+}$ and *Nlrp3*$^{-/-}$ mice.[18] We confirmed deletion of NLRP3 protein in hearts from *Nlrp3*$^{-/-}$ mice by Western blot analysis (Figure S2A). In the absence of pressure overload, cardiac function and morphology did not differ between *Nlrp3*$^{+/+}$ and *Nlrp3*$^{-/-}$ mice (Figure 1E and 1F and Figure S2B). In *Nlrp3*$^{+/+}$ mice, pressure overload induced cardiac hypertrophy with preserved contractile function until day 14 (adaptive phase) and heart failure at day 28 after TAC (Figure 1E and Figure S2B). On the other hand, *Nlrp3*$^{-/-}$ hearts showed attenuated cardiac hypertrophy, but greater left ventricular dilation with impaired contractile function compared with *Nlrp3*$^{+/+}$ hearts in the adaptive phase after TAC (Figure 1E and Figure S2B). In the heart-failure phase, cardiac function and chamber size were similar between *Nlrp3*$^{+/+}$ and *Nlrp3*$^{-/-}$ hearts, whereas cardiac hypertrophy remained attenuated in *Nlrp3*$^{-/-}$ hearts (Figure 1E). Histological assessment demonstrated significantly smaller cardiomyocytes, and

reduced cardiac fibrosis and macrophage infiltration in *Nlrp3*$^{-/-}$ hearts compared with *Nlrp3*$^{+/+}$ hearts during pressure overload (Figure 1F and Figure S2C-S2F). In the adaptive phase, angiogenesis was suppressed in *Nlrp3*$^{-/-}$ hearts (Figure 1F and Figure S2F). Mortality after TAC was higher in *Nlrp3*$^{-/-}$ mice than in *Nlrp3*$^{+/+}$ mice (Figure 1G), whereas all sham-operated *Nlrp3*$^{+/+}$ and *Nlrp3*$^{-/-}$ mice survived (n=8 for each). All deaths of *Nlrp3*$^{-/-}$ mice were observed in the adaptive phase. Hemodynamic measurement revealed higher left ventricle end-diastolic pressure (LVEDP) and smaller absolute values of maximum and minimum dp/dt in *Nlrp3*$^{-/-}$ mice than in *Nlrp3*$^{+/+}$ mice after 14 days of pressure overload, while blood pressure in the ascending aorta was similar between these mice (Figure 1H). There were no significant differences in hemodynamic parameters between *Nlrp3*$^{+/+}$ and *Nlrp3*$^{-/-}$ mice at 28 days after TAC or sham operation (Figure S2G). Collectively, these results indicate that genetic disruption of NLRP3 prevented pathological cardiac remodeling, but might have impaired cardiac adaptative response to pressure overload.

Consistently, at 14 days after TAC, the mRNA levels of hypertrophic marker genes (*Nppa* and *Myh7*), a fibrosis-related gene (*Col1a1*), an angiogenesis-related gene (*Vegfa*), and inflammation-related genes (*Il1b*, *Il6*, *Tnfa*, and *Mcp1*) were upregulated in wild-type hearts, whereas they were suppressed in *Nlrp3*$^{-/-}$ hearts (Figure 2A). Caspase-1 activity and cleaved caspase-1 and IL-1β levels were lower in *Nlrp3*$^{-/-}$ hearts than in wild-type hearts (Figure 2B-2D). Mitochondrial dysfunction is one of the characteristics of failing cardiomyocytes. To examine mitochondrial function, we assessed mitochondrial DNA (mtDNA) content and oxidative damage and expression levels of genes associated with mitochondrial oxidative phosphorylation (OXPHOS) in the heart (Figure 2E and Figure S3).[23] While *Nlrp3*$^{+/+}$ failing hearts showed the decrease in mtDNA content and expression levels of some of OXPHOS genes and the increase in

mtDNA oxidative damage, no significant changes in these indicators of mitochondrial function were observed in *Nlrp3*$^{-/-}$ hearts during pressure overload. These results indicate that mitochondrial function during pressure overload was not impaired in *Nlrp3*$^{-/-}$ hearts. Thus, contractile dysfunction in *Nlrp3*$^{-/-}$ mice during pressure overload might not be due to pathological changes of cardiomyocytes, but be due to insufficient hemodynamic adaptation to pressure overload.

To dissect the role of NLRP3 in immune cells from that in non-immune cells, we performed bone marrow transplantation experiment (Figures 2F and 2G and Figure S4). Caspase-1 activation and IL-1β production in the heart did not differ between wild-type mice transplanted with *Nlrp3*$^{+/+}$ and *Nlrp3*$^{-/-}$ bone marrow during pressure overload (Figure 2F and 2G and Figure S4A). Both mice showed cardiac hypertrophy with preserved contractile function after 14 days of TAC to a similar extent (Figure S4B and S4C). Consistently, cardiomyocyte hypertrophy, fibrosis, macrophage infiltration, and angiogenesis in pressure-overloaded hearts were similar between wild-type mice with *Nlrp3*$^{+/+}$ and *Nlrp3*$^{-/-}$ bone marrow (Figure S4D-S4G). No significant differences in hemodynamic parameters were observed between these mice (Figure S4H). Collectively, these data indicate that NLRP3 inflammasome activation in cardiac non-immune cells initiates inflammation and adaptive cardiac hypertrophy in response to pressure overload.

ATP/P2X7 Axis Contributes to NLRP3 Inflammasome Activation and Cardiac Hypertrophy During Pressure Overload

Three models of NLRP3 inflammasome activation have been widely suggested: potassium efflux via the P2X7 purinergic receptor stimulated by extracellular ATP, reactive oxygen species

(ROS)-dependent dissociation of thioredoxin-interacting protein (TXNIP) from thioredoxin, and cathepsin B release through lysosomal rupture due to mechanical insult by crystalline ligands.[24] We focused on the first mechanism because during pressure overload, TXNIP level was not upregulated in the heart (Figure S5A) and crystalline ligands are considered not to be produced.

To investigate the involvement of extracellular ATP and the P2X7 receptor in NLRP3 inflammasome activation and cardiac hypertrophy, we induced pressure overload in wild-type mice treated with an ATP diphosphohydrolase, apyrase,[25] and *P2rx7*$^{-/-}$ mice. In these mice, caspase-1 activation and IL-1β production were suppressed during pressure overload compared with wild-type mice treated with vehicle or *P2rx7*$^{+/+}$ mice (Figure 3A-3D and Figure S5B and S5C). We also found attenuated cardiac hypertrophy, greater ventricular dilation and contractile dysfunction with smaller cardiomyocytes, reduced cardiac fibrosis and macrophage infiltration, and lower capillary density in these mice compared with control mice on day 14 after TAC (Figure 3E and 3F and Figure S5D, S5E, and S6A-S6H). Hemodynamic measurement showed that apyrase treatment or genetic disruption of the P2X7 receptor led to higher LVEDP and smaller maximum dp/dt in pressure-overloaded hearts without affecting blood pressure in the ascending aorta (Figure S6I and S6J). These data indicate that extracellular ATP and the P2X7 receptor are required for NLRP3 inflammasome activation and adaptive cardiac hypertrophy in response to pressure overload.

Role of ATP/P2X7 Axis in the Heart

To clarify the role of the ATP/P2X7 axis and the NLRP3 inflammasome in cardiac cells, we assessed their impact on cardiomyocyte hypertrophy and proliferation of fibroblasts and vascular endothelial cells, which are important processes in cardiac hypertrophy.[2,4] We have previously

shown that TLR2 signaling is essential for IL-1β mRNA production in the stressed heart.[4] A specific ligand for TLR2, Pam3CSK4,[4] induced cardiomyocyte hypertrophy and proliferation of fibroblasts and vascular endothelial cells (Figure 3G-3I). Treatment with ATP in combination with Pam3CSK4 resulted in further hypertrophy and proliferation. Pharmacological inhibition of the P2X7 receptor, *Nlrp3* knockdown, or anti-IL-1β neutralization antibody treatment inhibited the synergistic effects of ATP and Pam3CSK4 on cardiomyocytes, fibroblasts, and vascular endothelial cells (Figure 3G-3I and Figure S7). These data indicate that the ATP/P2X7 axis contributes to hypertrophic responses of cardiac cells through the NLRP3 inflammasome activation and IL-1β production.

We next examined whether activation of the P2X7 receptor, with or without an inflammasome priming signal, induces cardiac hypertrophy *in vivo*. Wild-type mice treated with a combination of BzATP, a P2X7 receptor agonist, and LPS, a ligand of TLR4, for 14 days showed cardiac hypertrophy and increased myocardial caspase-1 activity and IL-1β level with preserved systolic function and chamber size, compared with those treated with vehicle (Figure S8A-S8C). Histological assessment demonstrated cardiomyocyte hypertrophy and augmented interstitial fibrosis in wild-type mice treated with the combination (Figure S8D-S8F), which was confirmed by the increase in expression levels of *Myh7* and *Col1a1*(Figure S8G-S8I). At our dose, BzATP or LPS alone did not induce cardiac hypertrophy (Figure S8A). Treatment with BzATP alone increased myocardial caspase-1 activity, but to a lesser extent than the combination treatment, which did not lead to IL-1β production (Figure S8B and S8C). Treatment with MCC950, a potent and specific NLRP3 inhibitor, or anti-IL-1β antibodies inhibited caspase-1 activation, IL-1β production, and cardiac hypertrophy without affecting systolic function or chamber size in wild-type mice treated with the combination of BzATP and LPS, compared with

control treatment (Figure S8A-S8I). Blood pressure was not affected by these treatments (Figure S8J). The P2X7 receptor has been implicated in cardiomyocyte hypertrophy and cellular survival through NLRP3 inflammasome-independent mechanisms.[26] Our data suggest that P2X7 receptor signaling might regulate cardiac hypertrophic changes *in vivo* mainly through the NLRP3 inflammasome activation and IL-1β production, rather than through NLRP3 inflammasome-independent mechanisms. In addition, IL-1β might affect myocardial caspase-1 activity in a positive-feedback manner through NF-κB activation.

SENs Release ATP for NLRP3 Inflammasome Activation

To examine the dynamics of extracellular ATP during pressure overload, we measured its concentration in the heart with an ATP-sensing electrode (Figure 4A and Figure S9A).[27] We found that extracellular ATP was increased in wild-type hearts on day 14 after TAC compared with sham-operated mice, whereas apyrase treatment reduced its concentration (Figure 4B and Figure S9B-S9D). We also visualized extracellular ATP *in vivo* by expressing the engineered firefly luciferase, called pmeLUC, which localizes to the outer aspect of the plasma membrane with the catalytic site facing the extracellular environment,[28] in cardiomyocytes through the use of adeno-associated virus, and confirmed the increase of extracellular ATP by pressure overload (Figures 4C-4F). As a danger signal, ATP is released by necrotic or apoptotic cells in damaged organs. In the pressure-overloaded heart, however, massive cell death does not occur; thus, extracellular ATP may be released by active transport from living cells. It is reported that cardiac cells can release ATP only below a physiologically active concentration.[29] Because ATP is a neurotransmitter and is secreted from nerve terminals,[30] we hypothesized that the autonomic nervous system may be the main source of extracellular ATP for NLRP3 inflammasome

activation in the heart during pressure overload.

We first examined the role of the sympathetic nervous system (SNS), which innervates the left ventricle more abundantly than does the parasympathetic nervous system, in ATP release and NLRP3 inflammasome activation in the pressure-overloaded heart.[31] Immunohistochemistry confirmed the presence of catecholaminergic nerve fibers in the epicardial nerve bundles around the left ventricle (Figure 4G). No significant difference in total areas of epicardial catecholaminergic nerve fibers was observed between sham-operated and TAC-operated hearts at day 14 after the operations. We measured extracellular ATP level in the left ventricle of wild-type mice treated with ablation of the left stellate ganglion,[20] the main source of the SEN terminals in the left ventricle, and clonidine, a SNS suppressant through stimulation of the α2-adrenergic receptor in the central nervous system (CNS). In these mice, extracellular ATP level during pressure overload was suppressed compared with wild-type mice without any treatment (Figure 4B and Figure S9E and S9F). In addition, these mice showed impairment of the cardiac adaptive response to pressure overload, with suppressed caspase-1 activation and IL-1β production, while systolic blood pressure was not affected by ablation of the left stellate ganglionectomy or clonidine treatment (Figure 4H-4K and Figure S10 and S11). These data indicate that SEN signals to the heart are required for the increase of extracellular ATP level and NLRP3 inflammasome activation to induce cardiac adaptive hypertrophy during pressure overload. In addition, it is suggested that the CNS is involved in this mechanism.

Next, we investigated whether SNS activation is sufficient for the increase of extracellular ATP level and NLRP3 inflammasome activation in the heart. Sympathetic activation by pseudoephedrine increased extracellular ATP level and caspase-1 activity in wild-type hearts (Figure 4B and 4L and Figure S9G and S12A). In pseudoephedrine-treated *Nlrp3*$^{-/-}$ hearts,

caspase-1 activation was suppressed compared with that in pseudoephedrine-treated wild-type hearts (Figure 4L and Figure S12A). We didn't find significant differences in systolic blood pressure and heart rate between pseudoephedrine-treated *Nlrp3*$^{+/+}$ and *Nlrp3*$^{-/-}$ mice, while pseudoephedrine slightly increased systolic blood pressure in these mice compared with vehicle (Figure S12B and S12C). Thus, sympathetic activation induces extracellular ATP release and NLRP3 inflammasome-dependent caspase-1 activation in the heart.

At our dose, pseudoephedrine did not induce IL-1β production and cardiac hypertrophy in both wild-type and *Nlrp3*$^{-/-}$ mice, although pseudoephedrine slightly increased macrophage infiltration (Figure 4L and Figure S12D-S12I). These findings suggest that NLRP3 inflammasome activation by the SNS alone might not be sufficient for IL-1β production. Other signaling pathways such as TLR signaling, which upregulates IL-1β mRNA, might be necessary for IL-1β production and cardiac hypertrophy.

We next investigated the impact of adrenergic signals on extracellular ATP level and NLRP3 inflammasome activation in the heart. Infusion of isoproterenol, a β-adrenergic receptor agonist, induced cardiac hypertrophy with fibrosis, macrophage infiltration and angiogenesis in both wild-type and *Nlrp3*$^{-/-}$ mice (Figure 4M and Figure S13A-S13F). No significant differences in systolic blood pressure and heart rate were observed between isoproterenol-treated *Nlrp3*$^{+/+}$ and *Nlrp3*$^{-/-}$ mice, while isoproterenol slightly increased systolic blood pressure and heart rate compared with vehicle (Figure S13G and S13H). Norepinephrine, a main neurotransmitter of the SENs, induced cardiomyocyte hypertrophy and proliferation of cardiac fibroblasts and vascular endothelial cells in an NLRP3 inflammasome-independent manner *in vitro* (Figure S14). Isoproterenol did not significantly increase extracellular ATP level in the heart (Figure 4B and Figure S9H). Caspase-1 activity and cleaved caspase-1 level were increased in both

isoproterenol-treated wild-type and *Nlrp3*$^{-/-}$ mice (Figure 4M and Figure S13I). Interestingly, IL-1β level was not increased in these mice (Figure 4M). Collectively, these data suggest that in the pressure-overloaded heart, ATP might be released mainly from SEN terminals rather than from cardiac cells, stimulated by adrenergic signals. In addition, adrenergic signals might be able to induce caspase-1 activation and cardiac hypertrophy in an NLRP3 inflammasome-independent manner.

ATP released from the sympathetic nerve terminals has been reported to modulate presynaptic norepinephrine release through activation of purinergic receptors.[32,33] To examine the impact of extracellular ATP on presynaptic norepinephrine release and the role of norepinephrine on NLRP3 inflammasome activation and cardiac phenotype in the pressure-overloaded heart, we next measured myocardial and plasma norepinephrine levels. We found that pressure overload by TAC increases myocardial and plasma norepinephrine levels in wild-type mice (Figure S15). No significant differences in myocardial and plasma norepinephrine levels were detected between TAC-operated *Nlrp3*$^{+/+}$ and *Nlrp3*$^{-/-}$ mice. Apyrase treatment or genetic disruption of the P2X7 receptor did not affect norepinephrine level in the heart or plasma on day 14 after TAC or sham operation. We didn't observe the increase of myocardial norepinephrine level after TAC in wild-type mice treated with ablation of the left stellate ganglion, while this treatment didn't have an effect on plasma norepinephrine level, which might reflect the contribution of the left stellate ganglion to sympathetic innervation in the left ventricle. These data suggest that ATP might regulate presynaptic norepinephrine release with various positive and negative feedbacks through purinergic receptors, including P2X and P2Y receptors,[32] which might explain why myocardial norepinephrine level was not altered by ATP depletion or genetic disruption of the P2X7 receptor. In addition, our data indicate that norepinephrine might not contribute to NLRP3

inflammasome activation and cardiac phenotype in our TAC model. Furthermore, pressure overload might increase systemic sympathetic neural activity and norepinephrine in the blood, while the increase of norepinephrine in the pressure-overloaded heart might be attributable mainly to its release from the SEN terminals in the heart.

ATP from SENs Is Essential for Cardiac Hypertrophy

Vesicular nucleotide transporter (VNUT; also known as *Slc17a9*) is a secretory vesicle protein that is responsible for the storage and release of ATP in neurons.[34] To clearly dissect the role of ATP release from that of norepinephrine release by the SNS in the pressure-overloaded heart, we crossed mice bearing a *Slc17a9*^{flox} allele with transgenic mice expressing *Cre* recombinase under the control of the dopamine β-hydroxylase (DBH) promoter, in order to generate *Slc17a9*$^{flox/flox}$;DBH-*Cre*$^{+}$ (*Slc17a9*$^{-/-}$) mice.[19] The DBH promoter drives gene expression in noradrenergic and adrenergic cell groups including postganglionic neurons in the SNS (Figure 5A). In *Slc17a9*$^{-/-}$ mice, ATP release from SEN terminals is inhibited, whereas norepinephrine release remains intact. We used *Slc17a9*$^{flox/flox}$;DBH-*Cre*$^{-}$ (*Slc17a9*$^{+/+}$) littermates as controls. *Slc17a9*$^{-/-}$ mice did not display a cardiac structural or functional deficit at baseline. In *Slc17a9*$^{-/-}$ mice, extracellular ATP release, caspase-1 activation and IL-1β production in the heart were suppressed compared with those in *Slc17a9*$^{+/+}$ mice on day 14 after TAC (Figure 4B and 5B-5D and Figure S9I and S9J). Myocardial and plasma norepinephrine levels were comparable between *Slc17a9*$^{+/+}$ and *Slc17a9*$^{-/-}$ mice (Figure 5E and 5F). *Slc17a9*$^{-/-}$ mice showed attenuated cardiac hypertrophy and contractile dysfunction, with reduced cardiomyocyte hypertrophy, fibrosis, capillary density and macrophage infiltration compared with *Slc17a9*$^{+/+}$ mice, indicating impairment of the adaptive mechanisms in response to pressure overload (Figure 5G-5L).

Consistently, higher LVEDP and smaller maximum dp/dt in pressure-overloaded hearts were observed in *Slc17a9*$^{-/-}$ mice compared with *Slc17a9*$^{+/+}$ mice, although blood pressure in the ascending aorta was comparable between these mice (Figure 5M). Collectively, SEN signals directly regulate NLRP3 inflammasome activation and cardiac adaptive hypertrophy through ATP release.

Role of Cardiac Afferent Nerves in ATP Release from SENs and NLRP3 Inflammasome Activation

We next assessed whether afferent input signals from the heart contribute to ATP release from SENs and NLRP3 inflammasome activation. No significant difference in total areas of epicardial primary afferent nerve fibers was observed between sham-operated and TAC-operated hearts at day 14 after the operations (Figure 6A). We treated the heart with capsaicin, an agonist for the transient receptor potential vanilloid type 1 channel which is predominantly expressed on the terminals of primary sensory neurons, to ablate afferent nerves from the heart.[8,21] Consistently with the previous reports, immunohistochemical staining confirmed ablation of primary sensory nerve fibers without depletion of catecholaminergic nerve fibers (Figure 6B). Cardiac function and morphology did not differ between sham-operated wild-type mice treated with capsaicin or vehicle (Figures 6C-6H). Capsaicin-treated hearts showed reduced extracellular ATP level and suppressed caspase-1 activation and IL-1β production during pressure overload compared with vehicle-treated mice (Figure 4B and 6I-6K and Figure S9K). Ablation of cardiac afferent nerves attenuated cardiac hypertrophy, but resulted in greater LV dilation and impaired systolic function with higher LVEDP and smaller absolute values of maximum and minimum dp/dt on day 14 after TAC, while this treatment did not affect systolic blood pressure in the ascending aorta

(Figure 6C, 6D, and 6L). Histological assessment revealed reduced cardiomyocyte hypertrophy, interstitial fibrosis, capillary density and macrophage infiltration by capsaicin treatment during pressure overload (Figure 6E-6H). Thus, ablation of cardiac afferent nerves impaired adaptive cardiac hypertrophy. These data indicate that afferent nerve signals are required for ATP release from SEN terminals and NLRP3 inflammasome activation for cardiac adaptive hypertrophy during pressure overload.

NLRP3 Inflammasome Activity in Isolated Perfused Hearts *Ex Vivo*

To further examine the significance of neural signals in NLRP3 inflammasome activation in the pressure-overloaded heart, we performed *ex vivo* experiment using the Langendorff perfused heart model.[35] In this experimental model, input and output neural signals in the heart are completely ablated. We found no significant differences in caspase-1 activity and IL-1β production between hearts with and without pressure overload of approximately 40 mmHg for 60 minutes (Figure S16). Our data suggest that pressure overload itself might not be sufficient for NLRP3 inflammasome activation and IL-1β production, although our experiment could assess only short-term responses.

Bisoprolol Inhibits Extracellular ATP Release and NLRP3 Inflammasome Activation

Lipophilic β-adrenergic receptor blockers are used as standard therapy for cardiac remodeling and heart failure.[36] These drugs can cross the blood-brain barrier. To investigate the impact of lipophilic β-adrenergic receptor blockers on extracellular ATP release and NLRP3 inflammasome activation in the heart, we induced pressure overload in wild-type mice treated with a lipophilic β-adrenergic receptor blocker, bisoprolol, or vehicle. Our tested dose of bisoprolol lowered heart

rate, but did not change systolic blood pressure in wild-type mice (Figure 7A). We assessed extracellular ATP levels by using the pmeLUC system, and found that bisoprolol reduced extracellular ATP in TAC-operated hearts (Figure 7B and 7C). In bisoprolol-treated mice, caspase-1 activation and IL-1β production were suppressed during pressure overload compared with vehicle-treated mice (Figure 7D and 7E). We observed attenuated cardiac hypertrophy, greater ventricular dilation and reduced ejection fraction with smaller cardiomyocytes, reduced cardiac fibrosis and macrophage infiltration, and lower capillary density in bisoprolol-treated mice compared with control mice at day 14 after TAC (Figure 7F-7K). Interestingly, ejection fraction remained above 50% in bisoprolol-treated mice. These results indicate that bisoprolol ameliorated cardiac inflammation and pathological cardiac remodeling, possibly in part, by inhibiting extracellular ATP release from the sympathetic nerve terminals, although our tested dose of bisoprolol suppressed systolic function under persistent pressure overload.

DISCUSSION

In this study, we demonstrated that neural signals control cardiac inflammation and hypertrophy through NLRP3 inflammasome activation and IL-1β production during pressure overload (Figure 8). IL-1β is a key proinflammatory cytokine that contributes to the pathophysiology of hypertrophic heart disease.[4,11] Active IL-1β production is tightly controlled in a two-step process.[10] The first step upregulates the inactive precursor, pro-IL-1β, by promoting the transcription of IL-1β gene. The second step processes pro-IL-1β into active IL-1β by activating caspase-1. In the heart, the first step is activated by local proinflammatory mechanisms, in which DAMPs from damaged cardiac cells stimulate innate immune receptors for NF-κB activation in an autocrine and paracrine manner.[4,5] Our data show that the second step is regulated by the

nervous system, including the CNS, through NLRP3 inflammasome activation. Thus, both local mechanisms and organ communications are necessary for proinflammatory process in the heart. Together with the previous reports that showed the involvement of the CNS in the pathophysiology of heart disease,[8,21,37] our mechanism might link psychological distress to heart disease.[38]

Inflammation is a double-edged sword that has both protective and harmful effects under various pathological conditions.[39,40] In our study, genetic disruption of NLRP3 resulted in contractile dysfunction and hemodynamic maladaptation with high mortality after TAC, while it inhibited cardiac hypertrophy and progression of pathological cardiac remodeling during pressure overload. Recently, NLRP3 inflammasome inhibitors have been suggested to be effective for the treatment of cardiovascular disease.[12,15,41,42] Our findings suggest that similarly to β-adrenergic receptor blockers, careful titration of NLRP3 inflammasome inhibitors might be necessary for inhibition of pathological cardiac remodeling without hemodynamic maladaptation.

Our results suggest that ATP, rather than norepinephrine, might be the main neurotransmitter that initiates cardiac inflammation and hypertrophy, at least in the adaptive phase of pressure overload, although β-adrenergic signals in the heart might have an interaction with the NLRP3 inflammasome and contribute to pathological cardiac remodeling in both NLRP3 inflammasome-dependent and -independent manners. Taken together with the data on bisoprolol-treated mice, lipophilic β-adrenergic receptor blockers, which are used as standard therapy for cardiac remodeling and heart failure,[36] might act on the brain, as well as on the heart, to inhibit SNS signals and cardiac inflammation with its ability to cross the blood-brain barrier. Further studies are needed to clarify the cross-talk between NLRP3 inflammasome activation and

β-adrenergic signals in hypertensive heart disease.

In conclusion, NLRP3 inflammasome activation through heart-brain interaction initiates cardiac inflammation and hypertrophy during pressure overload. The nervous system could be a therapeutic target for the treatment of hypertensive heart disease, although fine-tuning might be necessary.

For a comprehensive discussion of the study, see the Expanded Discussion in the Supplemental Material.

Acknowledgments

We are grateful to Dr. Jurg Tschopp (The University of Lausanne, Switzerland) and Dr. Francesco Di Virgilio (The University of Ferrara, Italy) for providing *Nlrp3*$^{-/-}$ mice and the plasmid harboring pmeLUC, respectively. Y.H. and M.S. conceived the study. Y.H. designed and performed experiments, and analyzed data. W.L. and Y.T. assisted with animal experiments and data analysis. G.N. and E.T. established and performed the Langendorff heart experiment. K.T., D.F. and Y.H. assisted with histological analysis, and discussed analyses and results of all experiments. T.I. assisted with the analysis of human samples. I.K. and M.S. supervised the research and provided scientific guidance and analysis. Y.H. and M.S. wrote the manuscript with input from all authors. All authors approved the manuscript.

Sources of Funding

This work was supported by a Japan Heart Foundation/Novartis Grant for Research Award on Molecular and Cellular Cardiology (to Y.H.), research grants from the Japan Foundation for Applied Enzymology (to Y.H.), the Cardiovascular Research Fund (to Y.H.), the Okinaka

Memorial Institute for Medical Research (to Y.H.), the Fugaku Fund for Medical Pharmaceuticals (to Y.H.), the Takeda Science Foundation (to Y.H., D.F., and M.S.), the SENSHIN Medical Research Foundation (to D.F.), and the Vehicle Racing Commemorative Foundation (to M.S.), and JSPS KAKENHI Grants (Number JP25860586 and JP15K09133 to Y.H., Number JP19K08584 to D.F., and Number JP19H03654 to M.S.).

Disclosures

The authors declare no competing interests.

Supplemental Material

Expanded Methods

Expanded Discussion

Figures S1-S16

Table S1

REFERENCES

1. Frey N, Olson EN. Cardiac hypertrophy: the good, the bad, and the ugly. Annu Rev Physiol. 2003;65:45-79. doi: 10.1146/annurev.physiol.65.092101.142243
2. Heineke J, Molkentin JD. Regulation of cardiac hypertrophy by intracellular signalling pathways. Nat Rev Mol Cell Biol. 2006;7:589-600.
3. Mann DL. Innate immunity and the failing heart: the cytokine hypothesis revisited. Circ Res. 2015;116:1254-1268. doi: 10.1161/CIRCRESAHA.116.302317
4. Higashikuni Y, Tanaka K, Kato M, Nureki O, Hirata Y, Nagai R, Komuro I, Sata M. Toll-like receptor-2 mediates adaptive cardiac hypertrophy in response to pressure overload through interleukin-1beta upregulation via nuclear factor kappaB activation. J Am Heart Assoc. 2013;2:e000267. doi: 10.1161/JAHA.113.000267
5. Oka T, Hikoso S, Yamaguchi O, Taneike M, Takeda T, Tamai T, Oyabu J, Murakawa T, Nakayama H, Nishida K, et al. Mitochondrial DNA that escapes from autophagy causes inflammation and heart failure. Nature. 2012;485:251-255. doi: 10.1038/nature10992
6. Kawai T, Akira S. The role of pattern-recognition receptors in innate immunity: update on Toll-like receptors. Nat Immunol. 2010;11:373-384. doi: 10.1038/ni.1863
7. Epelman S, Liu PP, Mann DL. Role of innate and adaptive immune mechanisms in cardiac injury and repair. Nat Rev Immunol. 2015;15:117-129. doi: 10.1038/nri3800
8. Fujiu K, Shibata M, Nakayama Y, Ogata F, Matsumoto S, Noshita K, Iwami S, Nakae S, Komuro I, Nagai R, et al. A heart-brain-kidney network controls adaptation to cardiac stress through tissue macrophage activation. Nat Med. 2017;23:611-622. doi: 10.1038/nm.4326
9. Sano S, Oshima K, Wang Y, MacLauchlan S, Katanasaka Y, Sano M, Zuriaga MA,

Yoshiyama M, Goukassian D, Cooper MA, et al. Tet2-Mediated Clonal Hematopoiesis Accelerates Heart Failure Through a Mechanism Involving the IL-1beta/NLRP3 Inflammasome. J Am Coll Cardiol. 2018;71:875-886. doi: 10.1016/j.jacc.2017.12.037

10. Franchi L, Eigenbrod T, Munoz-Planillo R, Nunez G. The inflammasome: a caspase-1-activation platform that regulates immune responses and disease pathogenesis. Nat Immunol. 2009;10:241-247.

11. Honsho S, Nishikawa S, Amano K, Zen K, Adachi Y, Kishita E, Matsui A, Katsume A, Yamaguchi S, Nishikawa K, et al. Pressure-mediated hypertrophy and mechanical stretch induces IL-1 release and subsequent IGF-1 generation to maintain compensative hypertrophy by affecting Akt and JNK pathways. Circ Res. 2009;105:1149-1158.

12. Fuster JJ, MacLauchlan S, Zuriaga MA, Polackal MN, Ostriker AC, Chakraborty R, Wu CL, Sano S, Muralidharan S, Rius C, et al. Clonal hematopoiesis associated with TET2 deficiency accelerates atherosclerosis development in mice. Science. 2017;355:842-847. doi: 10.1126/science.aag1381

13. Kawaguchi M, Takahashi M, Hata T, Kashima Y, Usui F, Morimoto H, Izawa A, Takahashi Y, Masumoto J, Koyama J, et al. Inflammasome activation of cardiac fibroblasts is essential for myocardial ischemia/reperfusion injury. Circulation. 2011;123:594-604. doi: 10.1161/CIRCULATIONAHA.110.982777

14. Mezzaroma E, Toldo S, Farkas D, Seropian IM, Van Tassell BW, Salloum FN, Kannan HR, Menna AC, Voelkel NF, Abbate A. The inflammasome promotes adverse cardiac remodeling following acute myocardial infarction in the mouse. Proc Natl Acad Sci U S A. 2011;108:19725-19730. doi: 10.1073/pnas.1108586108

15. Suetomi T, Willeford A, Brand CS, Cho Y, Ross RS, Miyamoto S, Brown JH.

Inflammation and NLRP3 Inflammasome Activation Initiated in Response to Pressure Overload by Ca(2+)/Calmodulin-Dependent Protein Kinase II delta Signaling in Cardiomyocytes Are Essential for Adverse Cardiac Remodeling. Circulation. 2018;138:2530-2544. doi: 10.1161/CIRCULATIONAHA.118.034621

16. Xiao H, Li H, Wang JJ, Zhang JS, Shen J, An XB, Zhang CC, Wu JM, Song Y, Wang XY, et al. IL-18 cleavage triggers cardiac inflammation and fibrosis upon beta-adrenergic insult. Eur Heart J. 2018;39:60-69. doi: 10.1093/eurheartj/ehx261

17. Wang Y, Wu Y, Chen J, Zhao S, Li H. Pirfenidone attenuates cardiac fibrosis in a mouse model of TAC-induced left ventricular remodeling by suppressing NLRP3 inflammasome formation. Cardiology. 2013;126:1-11. doi: 10.1159/000351179

18. Martinon F, Petrilli V, Mayor A, Tardivel A, Tschopp J. Gout-associated uric acid crystals activate the NALP3 inflammasome. Nature. 2006;440:237-241. doi: 10.1038/nature04516

19. Matsushita N, Kobayashi K, Miyazaki J, Kobayashi K. Fate of transient catecholaminergic cell types revealed by site-specific recombination in transgenic mice. J Neurosci Res. 2004;78:7-15. doi: 10.1002/jnr.20229

20. Shimizu I, Yoshida Y, Katsuno T, Tateno K, Okada S, Moriya J, Yokoyama M, Nojima A, Ito T, Zechner R, et al. p53-induced adipose tissue inflammation is critically involved in the development of insulin resistance in heart failure. Cell Metab. 2012;15:51-64. doi: 10.1016/j.cmet.2011.12.006

21. Okada S, Yokoyama M, Toko H, Tateno K, Moriya J, Shimizu I, Nojima A, Ito T, Yoshida Y, Kobayashi Y, et al. Brain-derived neurotrophic factor protects against cardiac dysfunction after myocardial infarction via a central nervous system-mediated pathway.

Arterioscler Thromb Vasc Biol. 2012;32:1902-1909. doi: 10.1161/ATVBAHA.112.248930

22. Kanda Y. Investigation of the freely available easy-to-use software 'EZR' for medical statistics. Bone Marrow Transplant. 2013;48:452-458. doi: 10.1038/bmt.2012.244

23. Sato M, Kadomatsu T, Miyata K, Warren JS, Tian Z, Zhu S, Horiguchi H, Makaju A, Bakhtina A, Morinaga J, et al. The lncRNA Caren antagonizes heart failure by inactivating DNA damage response and activating mitochondrial biogenesis. Nat Commun. 2021;12:2529. doi: 10.1038/s41467-021-22735-7

24. Guo H, Callaway JB, Ting JP. Inflammasomes: mechanism of action, role in disease, and therapeutics. Nat Med. 2015;21:677-687. doi: 10.1038/nm.3893

25. Wilhelm K, Ganesan J, Muller T, Durr C, Grimm M, Beilhack A, Krempl CD, Sorichter S, Gerlach UV, Juttner E, et al. Graft-versus-host disease is enhanced by extracellular ATP activating P2X7R. Nat Med. 2010;16:1434-1438. doi: 10.1038/nm.2242

26. Shokoples BG, Paradis P, Schiffrin EL. P2X7 Receptors: An Untapped Target for the Management of Cardiovascular Disease. Arterioscler Thromb Vasc Biol. 2021;41:186-199. doi: 10.1161/ATVBAHA.120.315116

27. Gourine AV, Llaudet E, Dale N, Spyer KM. ATP is a mediator of chemosensory transduction in the central nervous system. Nature. 2005;436:108-111. doi: 10.1038/nature03690

28. Pellegatti P, Falzoni S, Pinton P, Rizzuto R, Di Virgilio F. A novel recombinant plasma membrane-targeted luciferase reveals a new pathway for ATP secretion. Mol Biol Cell. 2005;16:3659-3665. doi: 10.1091/mbc.e05-03-0222

29. Nishida M, Sato Y, Uemura A, Narita Y, Tozaki-Saitoh H, Nakaya M, Ide T, Suzuki K,

623 Inoue K, Nagao T, et al. P2Y6 receptor-Galpha12/13 signalling in cardiomyocytes
624 triggers pressure overload-induced cardiac fibrosis. EMBO J. 2008;27:3104-3115. doi:
625 10.1038/emboj.2008.237
626 30. Burnstock G. Historical review: ATP as a neurotransmitter. Trends Pharmacol Sci.
627 2006;27:166-176. doi: 10.1016/j.tips.2006.01.005
628 31. Kanazawa H, Ieda M, Kimura K, Arai T, Kawaguchi-Manabe H, Matsuhashi T, Endo J,
629 Sano M, Kawakami T, Kimura T, et al. Heart failure causes cholinergic
630 transdifferentiation of cardiac sympathetic nerves via gp130-signaling cytokines in
631 rodents. J Clin Invest. 2010;120:408-421. doi: 10.1172/JCI39778
632 32. Sperlagh B, Heinrich A, Csolle C. P2 receptor-mediated modulation of neurotransmitter
633 release-an update. Purinergic Signal. 2007;3:269-284. doi: 10.1007/s11302-007-9080-0
634 33. Li J, King NC, Sinoway LI. Interstitial ATP and norepinephrine concentrations in active
635 muscle. Circulation. 2005;111:2748-2751. doi:
636 10.1161/CIRCULATIONAHA.104.510669
637 34. Larsson M, Sawada K, Morland C, Hiasa M, Ormel L, Moriyama Y, Gundersen V.
638 Functional and anatomical identification of a vesicular transporter mediating neuronal
639 ATP release. Cereb Cortex. 2012;22:1203-1214. doi: 10.1093/cercor/bhr203
640 35. Takimoto E, Champion HC, Belardi D, Moslehi J, Mongillo M, Mergia E, Montrose DC,
641 Isoda T, Aufiero K, Zaccolo M, et al. cGMP catabolism by phosphodiesterase 5A
642 regulates cardiac adrenergic stimulation by NOS3-dependent mechanism. Circ Res.
643 2005;96:100-109. doi: 10.1161/01.RES.0000152262.22968.72
644 36. Bristow MR. beta-adrenergic receptor blockade in chronic heart failure. Circulation.
645 2000;101:558-569.

37. Leenen FH. Brain mechanisms contributing to sympathetic hyperactivity and heart failure. Circ Res. 2007;101:221-223. doi: 10.1161/CIRCRESAHA.107.158261

38. Jiang W, Kuchibhatla M, Cuffe MS, Christopher EJ, Alexander JD, Clary GL, Blazing MA, Gaulden LH, Califf RM, Krishnan RR, et al. Prognostic value of anxiety and depression in patients with chronic heart failure. Circulation. 2004;110:3452-3456. doi: 10.1161/01.CIR.0000148138.25157.F9

39. Ridker PM, Everett BM, Thuren T, MacFadyen JG, Chang WH, Ballantyne C, Fonseca F, Nicolau J, Koenig W, Anker SD, et al. Antiinflammatory Therapy with Canakinumab for Atherosclerotic Disease. N Engl J Med. 2017;377:1119-1131. doi: 10.1056/NEJMoa1707914

40. Gomez D, Baylis RA, Durgin BG, Newman AAC, Alencar GF, Mahan S, St Hilaire C, Muller W, Waisman A, Francis SE, et al. Interleukin-1beta has atheroprotective effects in advanced atherosclerotic lesions of mice. Nat Med. 2018;24:1418-1429. doi: 10.1038/s41591-018-0124-5

41. Zahid A, Li B, Kombe AJK, Jin T, Tao J. Pharmacological Inhibitors of the NLRP3 Inflammasome. Front Immunol. 2019;10:2538. doi: 10.3389/fimmu.2019.02538

42. Yao C, Veleva T, Scott L, Jr., Cao S, Li L, Chen G, Jeyabal P, Pan X, Alsina KM, Abu-Taha ID, et al. Enhanced Cardiomyocyte NLRP3 Inflammasome Signaling Promotes Atrial Fibrillation. Circulation. 2018;138:2227-2242. doi: 10.1161/CIRCULATIONAHA.118.035202

43. Nomura S, Satoh M, Fujita T, Higo T, Sumida T, Ko T, Yamaguchi T, Tobita T, Naito AT, Ito M, et al. Cardiomyocyte gene programs encoding morphological and functional signatures in cardiac hypertrophy and failure. Nat Commun. 2018;9:4435. doi:

669 10.1038/s41467-018-06639-7
670 44. Frey N, Katus HA, Olson EN, Hill JA. Hypertrophy of the heart: a new therapeutic
671 target? Circulation. 2004;109:1580-1589. doi: 10.1161/01.CIR.0000120390.68287.BB
672 45. Zhong Z, Liang S, Sanchez-Lopez E, He F, Shalapour S, Lin XJ, Wong J, Ding S, Seki E,
673 Schnabl B, et al. New mitochondrial DNA synthesis enables NLRP3 inflammasome
674 activation. Nature. 2018;560:198-203. doi: 10.1038/s41586-018-0372-z
675 46. Schultz HD, Ustinova EE. Capsaicin receptors mediate free radical-induced activation of
676 cardiac afferent endings. Cardiovasc Res. 1998;38:348-355. doi: 10.1016/s0008-
677 6363(98)00031-5
678 47. Scanzano A, Cosentino M. Adrenergic regulation of innate immunity: a review. Front
679 Pharmacol. 2015;6:171. doi: 10.3389/fphar.2015.00171
680 48. Rapacciuolo A, Esposito G, Caron K, Mao L, Thomas SA, Rockman HA. Important role
681 of endogenous norepinephrine and epinephrine in the development of in vivo pressure-
682 overload cardiac hypertrophy. J Am Coll Cardiol. 2001;38:876-882. doi: 10.1016/s0735-
683 1097(01)01433-4
684 49. Triposkiadis F, Karayannis G, Giamouzis G, Skoularigis J, Louridas G, Butler J. The
685 sympathetic nervous system in heart failure physiology, pathophysiology, and clinical
686 implications. J Am Coll Cardiol. 2009;54:1747-1762. doi: 10.1016/j.jacc.2009.05.015
687 50. Fukuda K, Kanazawa H, Aizawa Y, Ardell JL, Shivkumar K. Cardiac innervation and
688 sudden cardiac death. Circ Res. 2015;116:2005-2019. doi:
689 10.1161/CIRCRESAHA.116.304679
690

FIGURES

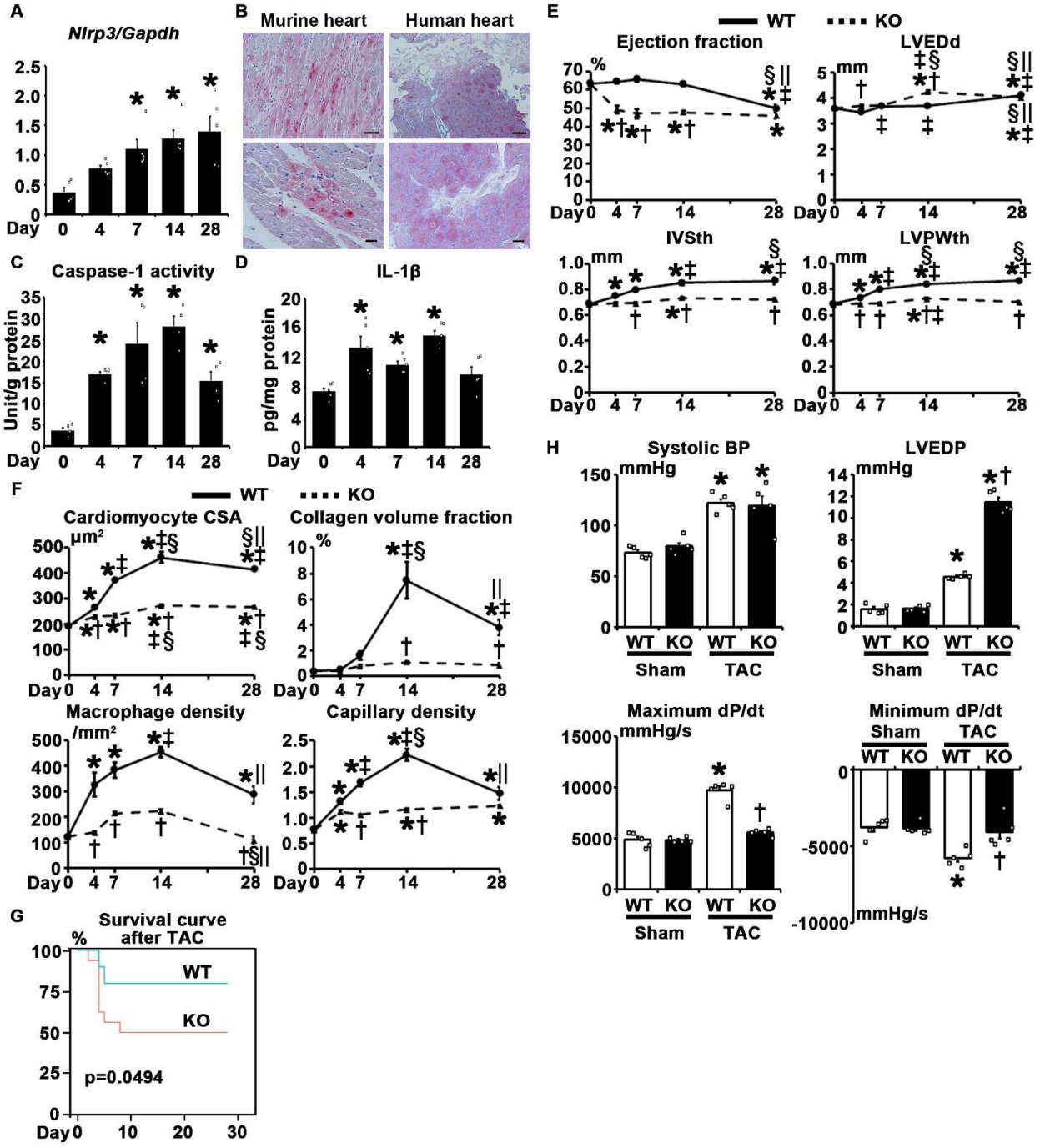

Figure 1. Genetic Disruption of NLRP3 Inhibits Adaptive Cardiac Hypertrophy.

A, Time course of *Nlrp3* gene expression during pressure overload in WT mice (n=5 per group). Quantitative RT-PCR was performed. Expression level of each gene was normalized to that of

Gapdh. **B,** Immunohistochemical staining for NLRP3 in wild-type murine heart subjected to 14 days of TAC and in human endomyocardial biopsy sample from heart failure patient. **C** and **D,** Caspase-1 activity (**C**, n=4 per group) and IL-1β protein level (**D**, n=5 per group) in pressure-overloaded WT hearts. IL-1β protein was detected by ELISA. Values were normalized to total protein level. **E,** Time course of echocardiographic parameters in wild-type (WT) and *Nlrp3* knockout (KO) mice during pressure overload (n=5 per group). IVSth, interventricular septum thickness; LVPWth, left ventricular posterior wall thickness; LVEDd, left ventricle end-diastolic diameter. **F,** Histological analysis of cardiomyocyte cross-sectional area (CSA), collagen volume fraction, macrophage density and capillary density in pressure-overloaded WT and KO hearts (n=5 per group). **G,** Survival curve after TAC operation in WT and KO mice (n=20 for WT mice; n=16 for KO mice). **H,** Hemodynamic parameters in WT and KO hearts subjected to sham or 14 days of TAC (n=5 per group). BP, blood pressure; LVEDP, left ventricle end-diastolic pressure. *P* values were calculated by one-way ANOVA with Dunnett's test (**A, C,** and **D**) or Holm test (**E**, **F**, and **H**) and Kaplan-Meier method with log-rank test (**G**). For **A**, **C**, and **D**, **P*<0.05 versus day 0. For **E** and **F**, **P*<0.05 versus day 0; †*P*<0.05 versus wild-type mice at the same time point; ‡*P*<0.05 versus day 4; §*P*<0.05 versus day 7; ‖*P*<0.05 versus day 14. For **H**, **P*<0.05 versus sham. †*P*<0.05 versus wild-type mice. All error bars represent S.E.M.

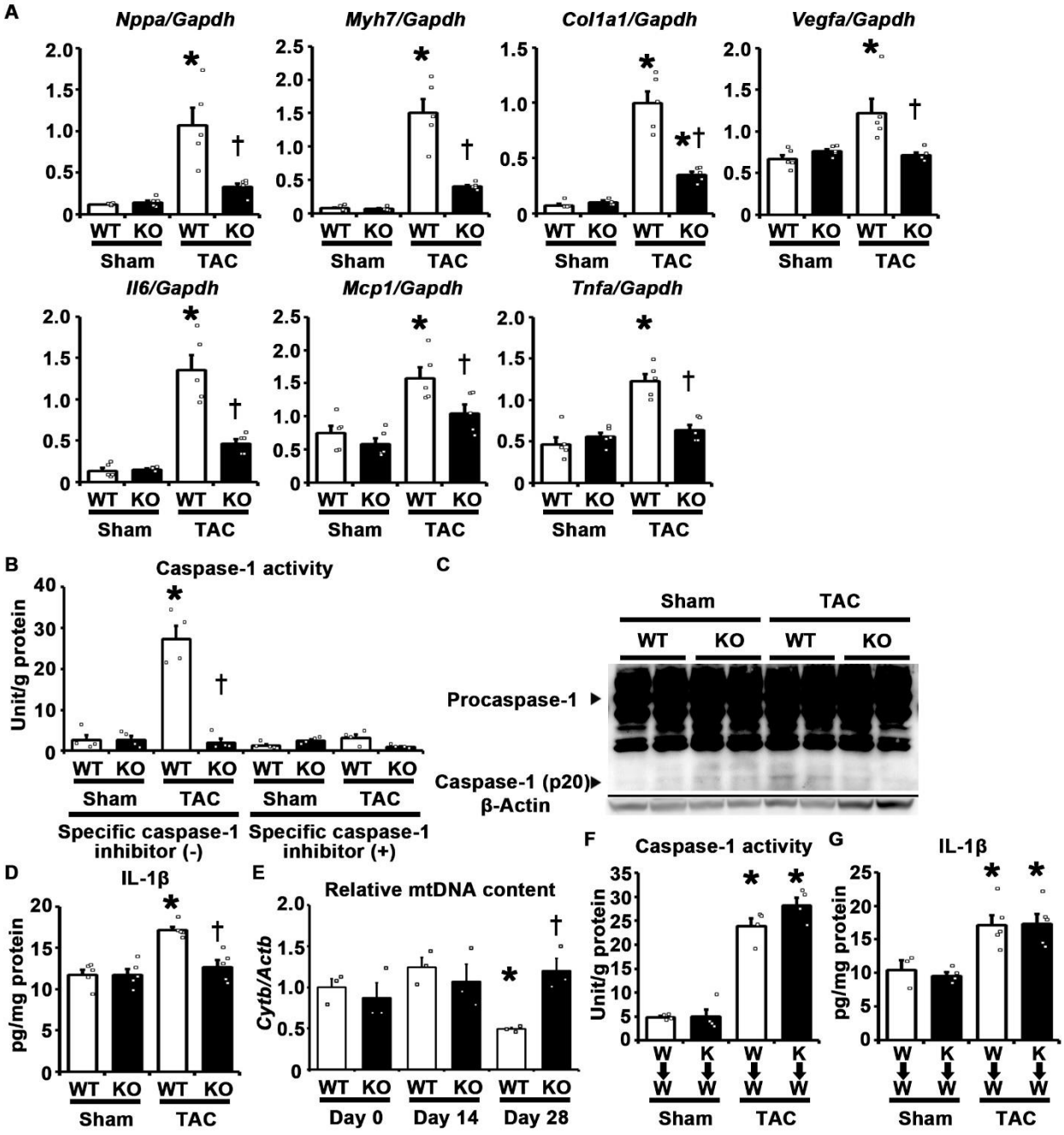

Figure 2. NLRP3 Inflammasome Activation Contributes to Pathological Cardiac Remodeling During Pressure Overload.

A, Expression levels of hypertrophic marker genes such as *Nppa* and *Myh7*, a fibrosis-related gene such as *Col1a1*, an angiogenesis-related gene such as *Vegfa*, and inflammation-related genes such as *Il6*, *Mcp1* and *Tnfa* in wild-type (WT) and *Nlrp3* knockout (KO) hearts. Mice were

subjected to sham or 14 days of TAC (n=5 per group). Expression level of each gene was determined by quantitative RT-PCR, and normalized to that of *Gapdh*. **B,** Caspase-1 activity with and without a specific caspase-1 inhibitor in pressure-overloaded hearts (n=4 per group). Values were normalized to total protein level. **C,** Western blot for procapase-1, cleaved caspase-1 (p20), and β-actin in pressure-overloaded hearts. **D,** IL-1β protein level in WT and KO hearts subjected to sham or 14 days of TAC (n=5 per group). IL-1β protein was detected by ELISA. Values were normalized to total protein level. **E,** Mitochondrial DNA (mtDNA) content in pressure-overloaded hearts (n=3 per group). DNA extracted from myocardial tissues was subjected to quantitative real-time PCR with specific primer sets for Cytochrome b (*Cytb*) (mtDNA) and β-actin (*Actb*) (nDNA). mtDNA to nDNA ratios were measured. **F** and **G**, Myocardial caspase-1 activity (**F**) and IL-1β protein level (**G**) in WT mice with WT bone marrow (W→W) or KO bone marrow (K→W) subjected to sham or 14 days of TAC. IL-1β protein was detected by ELISA. Values were normalized to total protein level. For **F**, n=4 per group. For **G**, n=3 for sham-operated W→W mice; n=4 for sham-operated K→W mice; n=5 for TAC-operated W→W and K→W mice. *P* values were calculated by one-way ANOVA with Holm test. For **A**, **B**, and **D**, **P*<0.05 versus sham. †*P*<0.05 versus WT mice. For **E**, **P*<0.05 versus day 14; †*P*<0.05 versus WT mice. For **F** and **G**, **P*<0.05 versus sham. All error bars represent S.E.M.

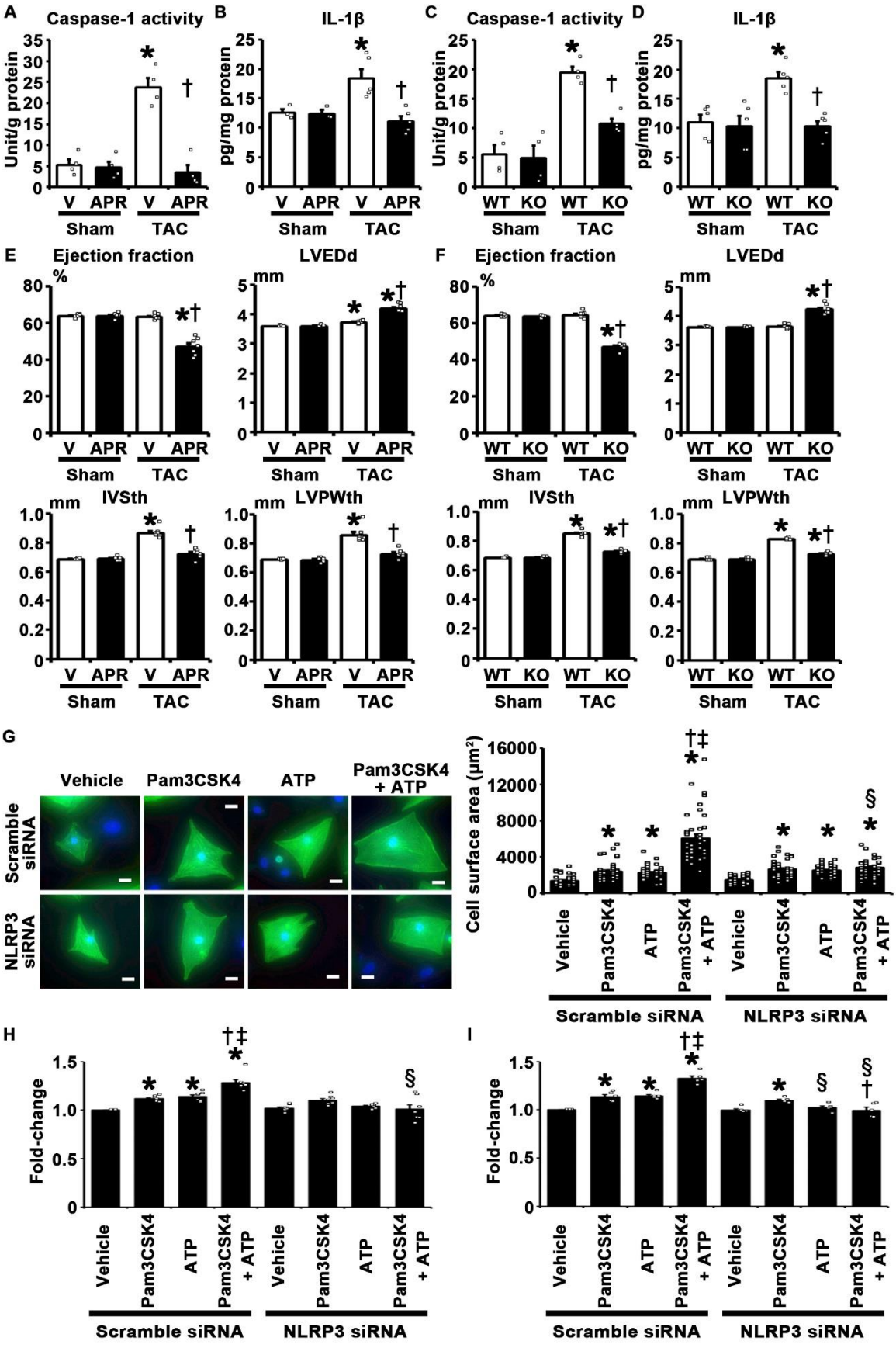
A
Caspase-1 activity
Unit/g protein
B
IL-1β
pg/mg protein
C
Caspase-1 activity
Unit/g protein
D
IL-1β
pg/mg protein
V APR V APR
Sham TAC
WT KO WT KO
Sham TAC
E
Ejection fraction
%
LVEDd
mm
IVSth
mm
LVPWth
mm
F
Ejection fraction
%
LVEDd
mm
IVSth
mm
LVPWth
mm
G
Vehicle
Pam3CSK4
ATP
Pam3CSK4 + ATP
Scramble siRNA
NLRP3 siRNA
Cell surface area (μm²)
Vehicle
Pam3CSK4
ATP
Pam3CSK4 + ATP
Scramble siRNA
NLRP3 siRNA
H
Fold-change
I
Fold-change

Figure 3. ATP/P2X7 Axis Is Involved in NLRP3 Inflammasome Activation and Cardiac Hypertrophy During Pressure Overload.

A and **B,** Caspase-1 activity (**A**) and IL-1β protein level (**B**) in vehicle-treated (V-treated) or apyrase-treated (APR-treated) wild-type (WT) hearts subjected to sham or 14 days of TAC. IL-1β protein was detected by ELISA. Values were normalized to total protein level. For **A**, n=4 per group. For **B**, n=3 for sham; n=5 for TAC. **C** and **D,** Caspase-1 activity (**C**) and IL-1β protein level (**D**) in WT and *P2rx7* knockout (KO) hearts subjected to sham or 14 days of TAC. For **C**, n=4 per group. For **D**, n=5 per group. **E** and **F,** Echocardiographic parameters in V- or APR-treated wild-type mice (n=6 for sham; n=7 for TAC) (**E**), and WT and KO mice (n=5 for sham; n=7 for TAC) (**F**). IVSth, interventricular septum thickness; LVPWth, left ventricular posterior wall thickness; LVEDd, left ventricle end-diastolic diameter. **G** through **I,** Cell surface area of cardiomyocytes after 48-hour stimulation (**G**) and proliferation of cardiac fibroblasts (**H**) and human microvascular endothelial cells from the heart (HMVEC-C) (**I**) after 24-hour stimulation with Pam3CSK4, ATP, or both under treatment with NLRP3 siRNA or scrambled siRNA. **G,** Cell surface area was measured in specimens by anti-sarcomeric α-actinin staining (n=40 per group). Scale bars=20μm. **H** and **I,** Cell proliferation was assessed by MTS (dimethylthiazol-carboxymethoxyphenyl-sulfophenyl-tetrazolium) assay. The percentage of the absorbance of wells with cells treated with scrambled siRNA or vehicle were calculated (n=7 per group for fibroblasts; n=5 per group for HMVEC-C). Data are expressed as a fold-change relative to the control group. *P* values were calculated by one-way ANOVA with Holm test. For **A** through **F**, **P*<0.05 versus sham. †*P*<0.05 versus vehicle-treated (V-treated) (**A**, **B**, and **E**) or WT (**C**, **D**, and **F**) mice. For **G** through **I**, **P*<0.05 versus vehicle; †*P*<0.05 versus Pam3CSK4; ‡*P*<0.05 versus ATP; §*P*<0.05 versus scrambled siRNA. All error bars represent S.E.M.

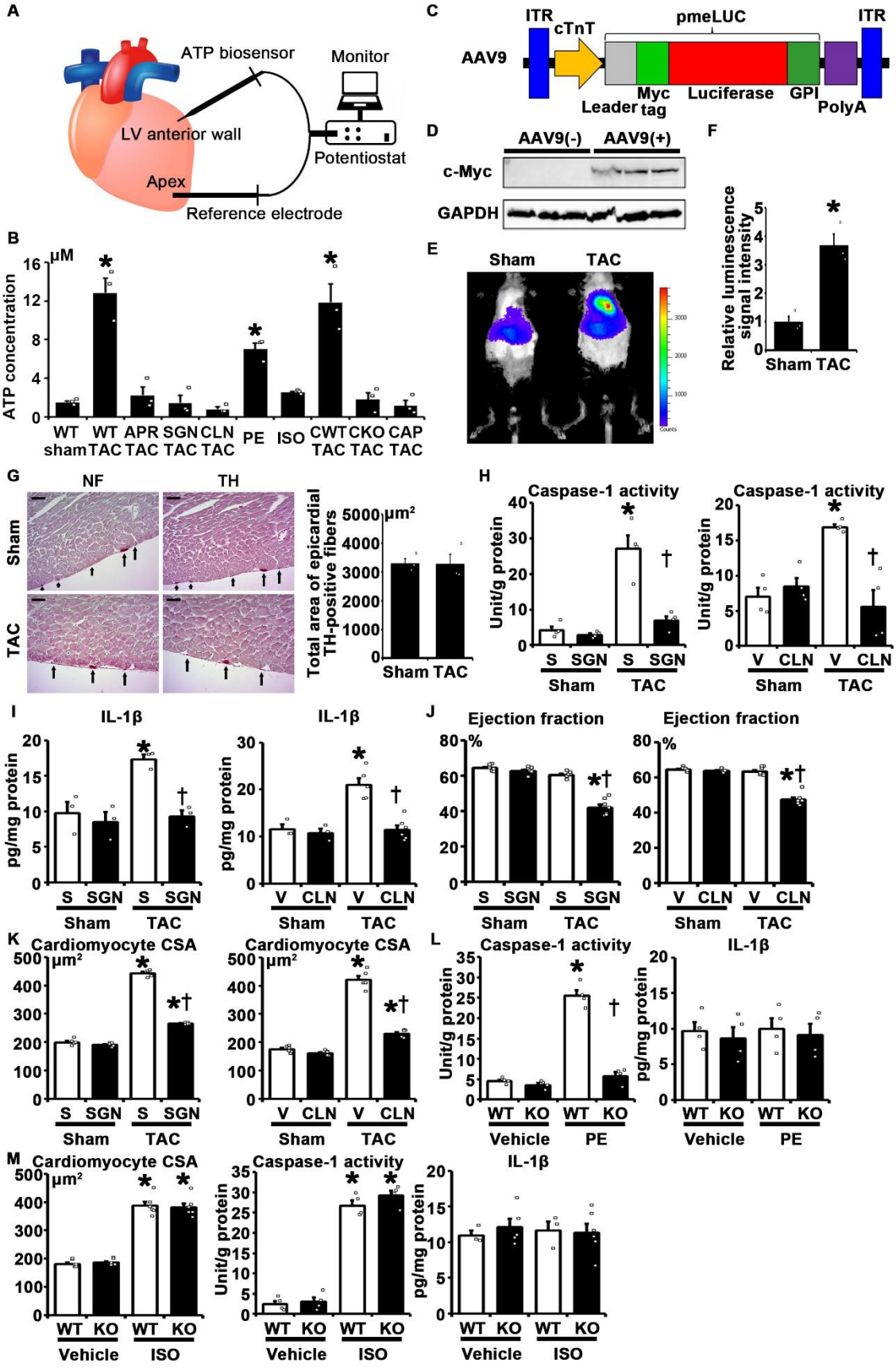
A
ATP biosensor
Monitor
LV anterior wall
Potentiostat
Apex
Reference electrode
B
μM
ATP concentration
WT sham
WT TAC
APR TAC
SGN TAC
CLN TAC
PE
ISO
CWT TAC
CKO TAC
CAP TAC
C
ITR
cTnT
pmeLUC
ITR
AAV9
Leader
Myc tag
Luciferase
GPI
PolyA
D
AAV9(-)
AAV9(+)
c-Myc
GAPDH
E
Sham
TAC
F
Relative luminescence signal intensity
Sham
TAC
G
NF
TH
Sham
TAC
Total area of epicardial TH-positive fibers
μm²
Sham
TAC
H
Caspase-1 activity
Unit/g protein
S
SGN
V
CLN
Sham
TAC
I
IL-1β
pg/mg protein
J
Ejection fraction
%
K
Cardiomyocyte CSA
μm²
L
Caspase-1 activity
IL-1β
WT
KO
Vehicle
PE
M
Cardiomyocyte CSA
Caspase-1 activity
IL-1β
Vehicle
ISO

762

Figure 4. SENs Release ATP for NLRP3 Inflammasome Activation.

A, Schematic of extracellular ATP measurement using enzyme-based biosensors. Electric current between the reference electrode and the ATP biosensor in the left ventricle (LV) was measured through a potentiostat and transformed into ATP level based on the calibration curve. **B,** Extracellular ATP level in the heart in sham-operated wild-type mice (WT sham), TAC-operated WT mice (WT TAC), TAC-operated mice with left stellate ganglionectomy (SGN TAC), pseudoephedrine-treated mice (PE), isoproterenol-treated mice (ISO), and TAC-operated mice treated with apyrase (APR TAC), clonidine (CLN TAC), or capsaicin (CAP TAC), *Slc17a9*$^{flox/flox}$;DBH-*Cre*$^{-}$ mice (CWT TAC), and *Slc17a9*$^{flox/flox}$;DBH-*Cre*$^{+}$ mice (CKO TAC) (n=3 mice per group). Mice were subjected to 14 days of treatment. **C,** Schematic of adeno-associated virus vector harboring an engineered firefly luciferase, called pmeLUC, that localizes to the outer aspect of the plasma membrane with the catalytic site facing the extracellular environment, in the downstream of the chicken cardiac troponin T promoter. This protein contains the Myc epitope tag. GPI, glycosylphosphatidylinositol; ITR, inverted terminal repeat. **D,** Western blot for pmeLUC and glyceradldehyde-3-phosphate dehydrogenase (GAPDH) in murine hearts with and without the transduction of AAV9 vector harboring pmeLUC. The pmeLUC protein was detected by anti-c-Myc antibody. **E** and **F,** Representative image (**E**) and data analysis (**F**) of extracellular ATP detection by the IVIS luminometer in WT hearts subjected to sham or 14 days of TAC. The average of luminescent signals within region of interest (i.e. the heart) was calculated for comparison (n=3 per group). **G,** Immunohistochemical staining for neurofilament (NF) and tyrosine hydroxylase (TH) in WT murine heart subjected to sham or 14 days of TAC with consecutive slices. Nerve fibers are stained by anti-NF antibody. Catecholaminergic nerve fibers are stained by anti-TH antibody. Total areas of epicardial TH-positive nerve fibers were

786 measured for comparison (n=3 per group). **H** through **K**, Myocardial caspase-1 activity (**H**) and
787 IL-1β protein level (**I**), ejection fraction (**J**), and cardiomyocyte cross-sectional area (CSA) (**K**)
788 in sham or TAC-operated mice with sham (S) or SGN and with vehicle (V) or CLN. **H,** n=4 per
789 group. **I,** For SGN experiment, n=3 per group. For CLN experiment, n=3 for sham; n=5 for V
790 TAC; n=6 for CLN TAC. **J,** For SGN experiment, n=7 per group. For CLN experiment, n=6 for
791 sham; n=7 for TAC. **K,** n=5 per group. **L,** Caspase-1 activity and IL-1β protein level in WT and
792 *Nlrp3* knockout (KO) hearts treated with vehicle or PE (n=4 per group). IL-1β protein was
793 detected by ELISA. Values were normalized to total protein level. **M,** Cardiomyocyte CSA (n=6
794 per group) and myocardial caspase-1 activity (n=4 per group) and IL-1β protein level (n=4 per
795 group) in WT and KO mice treated with vehicle or ISO. IL-1β protein was detected by ELISA.
796 Values were normalized to total protein level. *P* values were calculated by one-way ANOVA with
797 Holm test or unpaired two-tailed t-test. For **B**, **P*<0.05 versus WT sham. For **F**, **P*<0.05 versus
798 sham. For **H** through **K**, **P*<0.05 versus sham. †*P*<0.05 versus mice treated with S or V. For **L**
799 and **M**, **P*<0.05 versus vehicle. †*P*<0.05 versus WT mice. All error bars represent S.E.M.
800

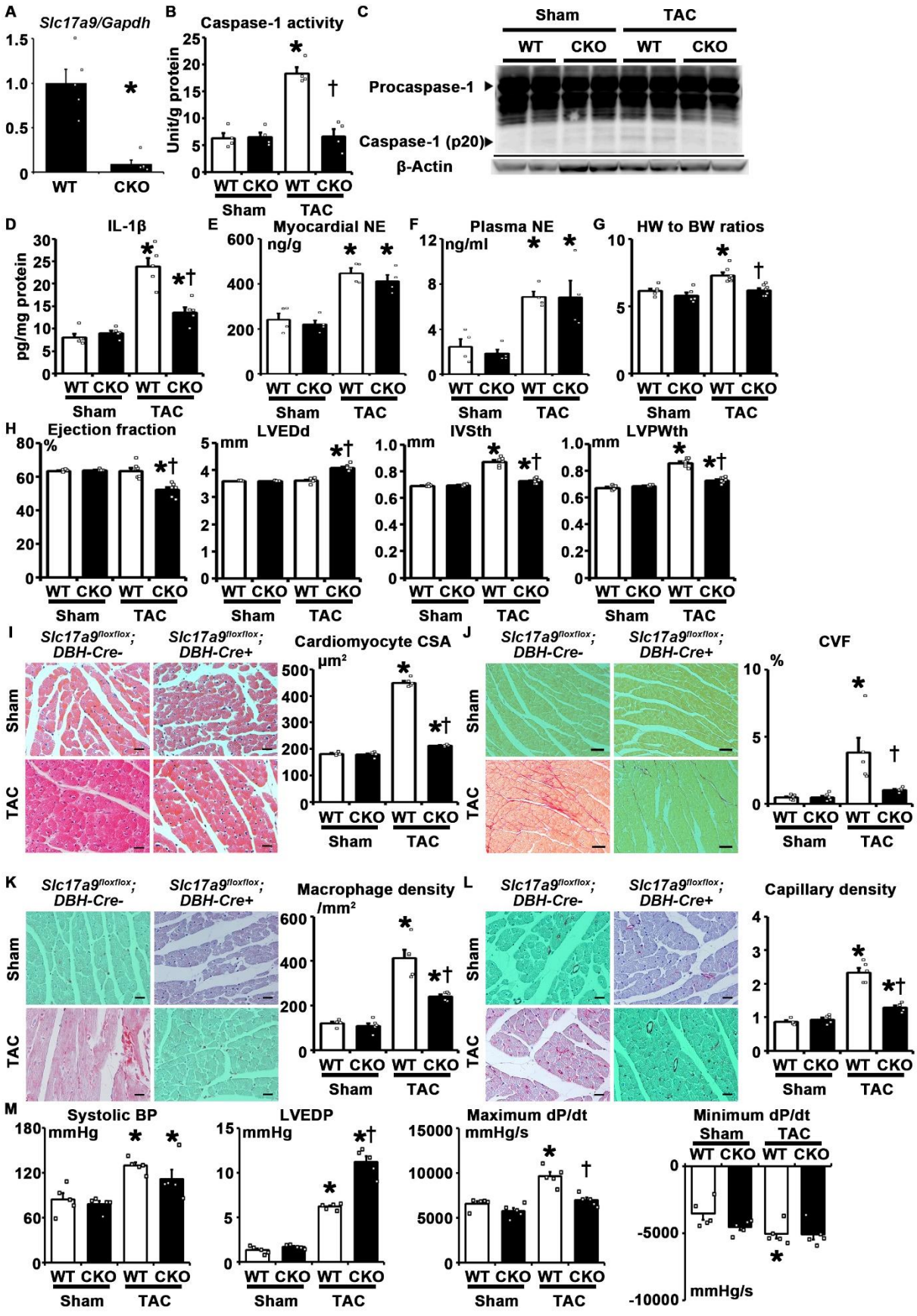
A
Slc17a9/Gapdh
B
Caspase-1 activity
Unit/g protein
C
Sham
TAC
WT
CKO
Procaspase-1
Caspase-1 (p20)
β-Actin
D
IL-1β
pg/mg protein
E
Myocardial NE
ng/g
F
Plasma NE
ng/ml
G
HW to BW ratios
H
Ejection fraction
%
LVEDd
mm
IVSth
LVPWth
I
Slc17a9floxflox; DBH-Cre-
Slc17a9floxflox; DBH-Cre+
Cardiomyocyte CSA
μm²
J
CVF
K
Macrophage density
/mm²
L
Capillary density
M
Systolic BP
mmHg
LVEDP
Maximum dP/dt
mmHg/s
Minimum dP/dt
Sham
TAC

801

Figure 5. ATP from SENs Is Essential for Cardiac Hypertrophy.

A, Gene expression of *Slc17a9* in left stellate ganglion of *Slc17a9*$^{flox/flox}$;DBH-*Cre*$^{-}$ (WT) and *Slc17a9*$^{flox/flox}$;DBH-*Cre*$^{+}$ (CKO) mice determined by quantitative RT-PCR (n=5 per group). Expression level of *Slc17a9* was normalized to that of *Gapdh*. **P*<0.05 versus WT mice. **B** through **M,** WT and CKO mice were subjected to sham or 14 days of TAC. **B,** Myocardial caspase-1 activity (n=4 per group). Values were normalized to total protein level. **C,** Western blot for procapase-1, cleaved caspase-1 (p20), and β-actin in the heart. **D,** Myocardial IL-1β protein level (n=5 per group). IL-1β protein was detected by ELISA. Values were normalized to total protein level. **E** and **F**, Myocardial and plasma norepinephrine (NE) concentration (n=4 per group). NE was detected by ELISA. Myocardial NE levels were normalized to tissue weight. **G,** Heart weight (HW) to body weight (BW) ratio (n=5 for sham; n=7 for TAC). **H,** Echocardiographic analysis of ejection fraction, left ventricle end-diastolic diameter (LVEDd), interventricular septum thickness (IVSth), and left ventricular posterior wall thickness (LVPWth) (n=5 for sham; n=7 for TAC). **I** through **L,** Histological analysis of cardiomyocyte cross-sectional area (CSA) (**I**), collagen volume fraction (CVF) (**J**), macrophage density (**K**) and capillary density (**L**) (n=5 for each group). Quantification of cardiomyocyte CSA and CVF was performed in specimens stained with hematoxylin and eosin or sirius red dye, respectively. Quantification of macrophage and capillary density was performed by immunohistochemical staining for Mac3 and CD31, respectively. Representative images are shown for each analysis. Scale bars=20μm for (**I**, **K**, and **L**). Scale bars=50μm for (**J**). **M,** Hemodynamic parameters (n=5 per group). BP, blood pressure; LVEDP, left ventricle end-diastolic pressure. *P* values were calculated by one-way ANOVA with Holm test. **P*<0.05 versus sham. †*P*<0.05 versus WT mice. All error bars represent S.E.M.

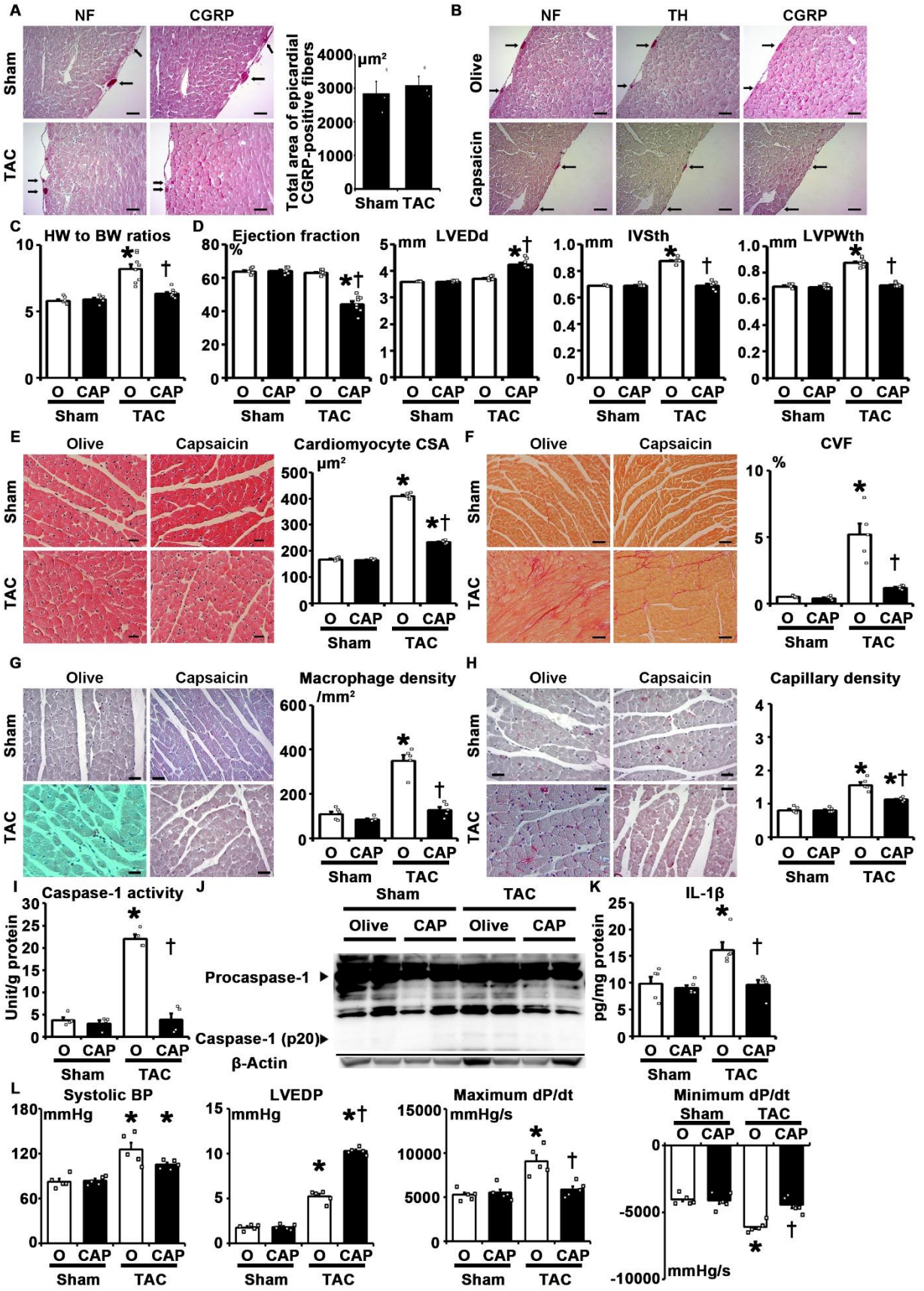
A
NF
CGRP
Sham
TAC
Total area of epicardial CGRP-positive fibers
μm²
Sham TAC
B
NF
TH
CGRP
Olive
Capsaicin
C
HW to BW ratios
O CAP O CAP
Sham TAC
D
Ejection fraction
%
LVEDd
mm
IVSth
mm
LVPWth
mm
E
Olive
Capsaicin
Cardiomyocyte CSA
μm²
F
CVF
%
G
Macrophage density
/mm²
H
Capillary density
I
Caspase-1 activity
Unit/g protein
J
Procaspase-1
Caspase-1 (p20)
β-Actin
K
IL-1β
pg/mg protein
L
Systolic BP
mmHg
LVEDP
mmHg
Maximum dP/dt
mmHg/s
Minimum dP/dt
mmHg/s

825

Figure 6. Role of Cardiac Afferent Nerves in ATP Release from SENs and NLRP3 Inflammasome Activation.

A, Immunohistochemical staining for neurofilament (NF) and calcitonin gene-related peptide (CGRP) in wild-type murine heart subjected to sham or 14 days of TAC with consecutive slices. Nerve fibers are stained by anti-NF antibody. Primary afferent nerve fibers are stained by anti-CGRP antibody. Total areas of epicardial CGRP-positive nerve fibers were measured for comparison (n=3 per group). **B,** Immunohistochemical staining for NF, tyrosine hydroxylase (TH), and CGRP in murine hearts treated with olive oil (O) or capsaicin (CAP) for ablation of the cardiac afferent nerves with consecutive slices. Catecholaminergic nerve fibers are stained by anti-TH antibody. **C** through **L,** Wild-type mice treated with O or CAP were subjected to sham or 14 days of TAC. **C,** Heart weight (HW) to body weight (BW) ratio (n=6 for sham; n=8 for TAC). **D,** Echocardiographic analysis of ejection fraction, left ventricle end-diastolic diameter (LVEDd), interventricular septum thickness (IVSth), and left ventricular posterior wall thickness (LVPWth) (n=6 for sham; n=8 for TAC). **E** through **H,** Histological analysis of cardiomyocyte cross-sectional area (CSA) (**E**), collagen volume fraction (CVF) (**F**), macrophage density (**G**) and capillary density (**H**) in the heart (n=5 for each group). Quantification of cardiomyocyte CSA and CVF was performed in specimens stained with hematoxylin and eosin or sirius red dye, respectively. Quantification of macrophage and capillary density was performed by immunohistochemical staining for Mac3 and CD31, respectively. Representative images are shown for each analysis. Scale bars=20μm for (**E**, **G**, and **H**). Scale bars=50μm for (**F**). **I,** Myocardial caspase-1 activity (n=4 per group). Values were normalized to total protein level. **J,** Western blot for procapase-1, cleaved caspase-1 (p20), and β-actin in the heart. **K,** Myocardial IL-1β protein level (n=5 per group). IL-1β protein was detected by ELISA. Values were

849 normalized to total protein level. **L,** Hemodynamic parameters (n=5 per group). BP, blood
850 pressure; LVEDP, left ventricle end-diastolic pressure. Values were normalized to total protein
851 level. *P* values were calculated by one-way ANOVA with Holm test or unpaired two-tailed t-test.
852 *$P<0.05$ versus sham. †$P<0.05$ versus wild-type mice treated with O. All error bars represent
853 S.E.M.
854

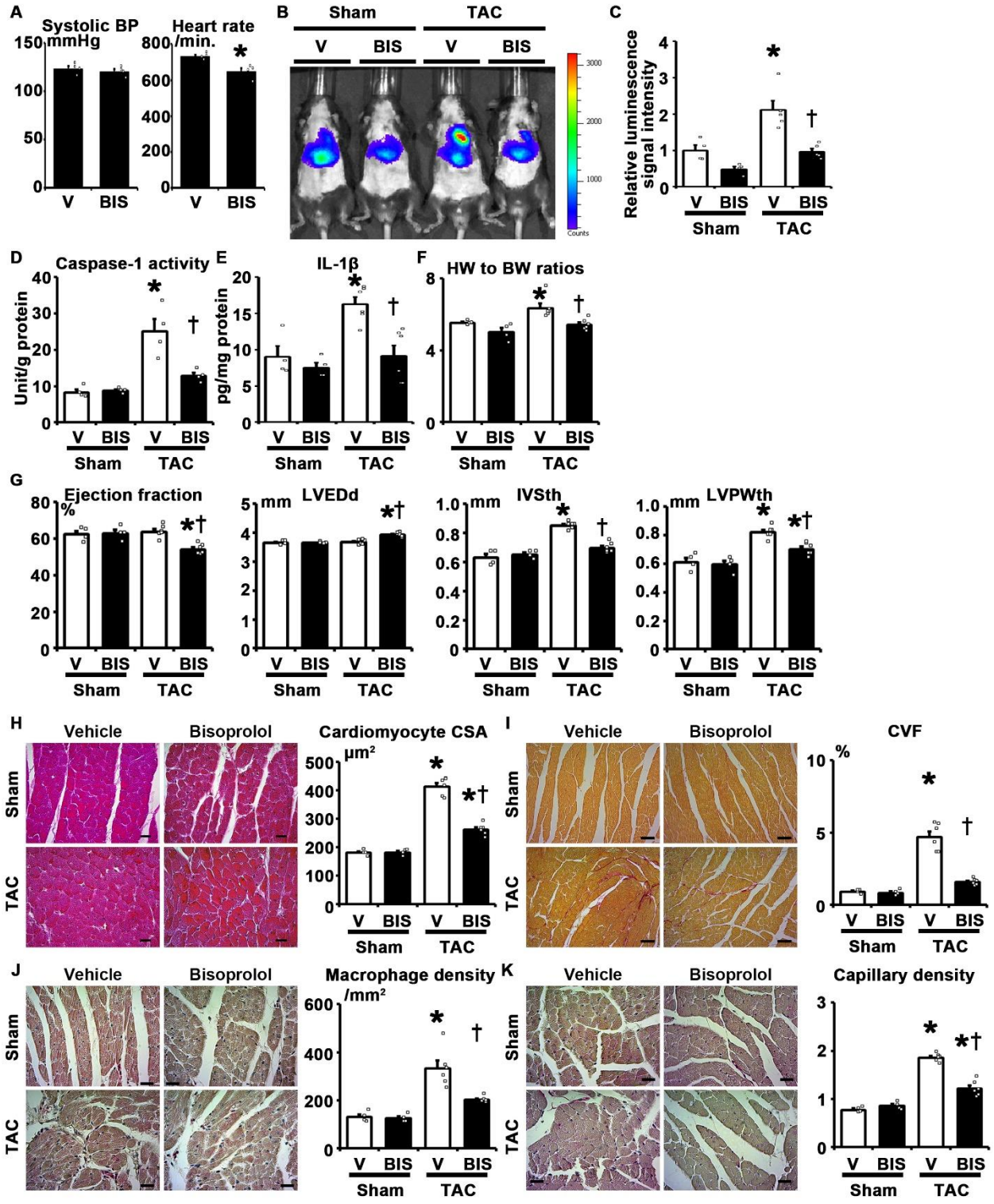

Figure 7. Bisoprolol Inhibits Extracellular ATP Release, NLRP3 Inflammasome Activation, and Cardiac Hypertrophy.

A, Systolic blood pressure (BP) and heart rate in wild-type mice treated with vehicle (V) or bisoprolol (BIS) for 14 days (n=4 per group). **B** through **K,** Wild-type mice treated with V or BIS were subjected to sham or 14 days of TAC. **B** and **C,** Representative image (**B**) and data analysis (**C**) of extracellular ATP detection by the IVIS luminometer. The average of luminescent signals within region of interest (i.e. the heart) was calculated for comparison (n=4 for sham; n=5 for TAC). **D** and **E,** Myocardial caspase-1 activity (**D**, n=4 per group) and IL-1β protein level (**E**, n=4 for sham; n=6 for TAC). IL-1β protein was detected by ELISA. Values were normalized to total protein level. **F,** Heart weight (HW) to body weight (BW) ratio (n=4 for sham; n=6 for TAC). **G,** Echocardiographic analysis of ejection fraction, left ventricle end-diastolic diameter (LVEDd), interventricular septum thickness (IVSth), and left ventricular posterior wall thickness (LVPWth) (n=4 for sham; n=6 for TAC). **H** through **K,** Histological analysis of cardiomyocyte cross-sectional area (CSA) (**H**), collagen volume fraction (CVF) (**I**), macrophage density (**J**) and capillary density (**K**) (n=4 for sham; n=6 for TAC). Quantification of cardiomyocyte CSA and CVF was performed in specimens stained with hematoxylin and eosin or sirius red dye, respectively. Quantification of macrophage and capillary density was performed by immunohistochemical staining for Mac3 and CD31, respectively. Representative images are shown for each analysis. Scale bars=20μm for (**H**, **J**, and **K**). Scale bars=50μm for (**I**). *P* values were calculated by one-way ANOVA with Holm test or unpaired two-tailed t-test. For **A**, **P*<0.05 versus V. For **C** through **K**, **P*<0.05 versus sham. †*P*<0.05 versus wild-type mice treated with V. All error bars represent S.E.M.

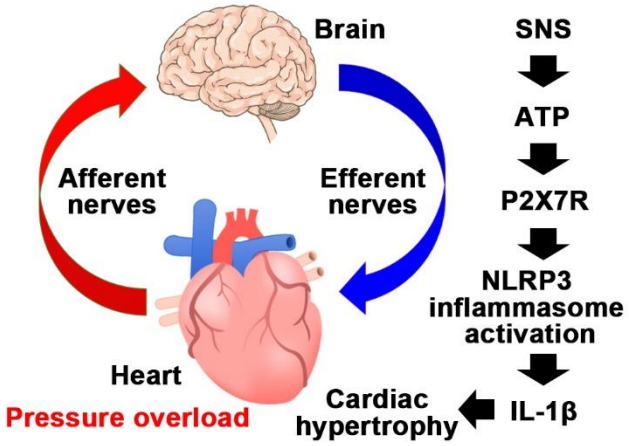

Figure 8. Proposed Regulatory Mechanism of Cardiac Inflammation and Homeostasis During Pressure Overload.

Pressure overload is sensed by cardiac afferent nerves to activate sympathetic efferent nerves (SENs) for ATP release, possibly via the central nervous system (CNS). ATP released from SEN terminals activates the NLRP3 inflammasome in cardiac non-immune cells through stimulation of the P2X7 receptor, which, together with TLR signaling, leads to IL-1β production to induce cardiac adaptive hypertrophy. Cardiac inflammation and homeostasis are controlled via heart-brain interaction.